Particle morphology and chemical microstructure of colloidal silica spheres made from alkoxysilanes

A. van Blaaderen [a] and A.P.M. Kentgens [b]

[a] *Van 't Hoff laboratory, University of Utrecht, Padualaan 8, 3584 CH Utrecht, The Netherlands*
[b] *SON-NWO HF-NMR Facility, University of Nijmegen, Toernooiveld, 6525 ED Nijmegen, The Netherlands*

Monodisperse colloidal silica spheres with radii in the range 10–500 nm were prepared by hydrolysis and condensation of tetraethoxysilane (TES) in a mixture of water, ammonia and a lower alcohol at several temperatures. It was attempted to establish a relation between the morphology and the chemical microstructure of the particle. Particle morphologies were examined with transmission electron microscopy and static and dynamic light scattering. The microstructure of the spheres was studied with quantitative direct excitation ^{29}Si nuclear magnetic resonance (NMR) spectroscopy and a combination of qualitative cross-polarization ^{13}C NMR and elemental analysis. A comparison was made between these particles and particles prepared from TES in an ammonia/water in cyclohexane microemulsion and also with Ludox $^{®}$ silica particles. The siloxane microstructure was found to show almost no variation as a function of concentration of reagents, catalyst, co-solvent and temperature. Around 65% of the silicon nuclei was bonded through siloxane bonds with four other silicons, approximately 30% was bonded with three other silicons and a few percent with only two. It was shown that under most experimental conditions several percent of the ethoxy groups never leave the TES molecule and end up inside the silica. The Ludox particles were found to consist of a more condensed silicon structure as compared with particles synthesized in alcohol, ammonia, water mixtures, whereas the spheres prepared in the microemulsion were less condensed and contained more alkoxy groups. The differences in particle morphologies – ranging from irregularly shaped rough particles to perfect, smooth spheres – are not caused by differences in siloxane and ethoxy microstructure. It is proposed instead, that a smooth and spherical particle shape is the result of the growth by monomers or small oligomers, and that a rough, irregular shape is the result of growth by larger silicon structures.

1. Introduction

Application of monodisperse silica spheres is of interest in many fields, including ceramics, glass preparation, catalysis, chromatography and colloids. Our interest in these particles stems from their use in physico-chemical studies of colloidal model systems. In many of these studies, use is being made of scattering techniques, such as light scattering, X-ray scattering and neutron scattering. The particle morphology (shape and

Correspondence to: Dr A. van Blaaderen, Van 't Hoff laboratory, University of Utrecht, Padualaan 8, 3584 CH, Utrecht, The Netherlands. Tel: +31-30 532 871. Telefax: +31-30 521 877.

surface roughness) and chemical structure and composition of the particle are important factors in these scattering experiments: light scattering is a result of the difference in refractive index of the particle and the solvent, X-ray scattering results from differences in electron density and neutron scattering results from differences in elemental density.

Another important factor that one wishes to control in studies of the properties of concentrated colloidal suspensions is the particle–particle interaction and the type of solvent in which the particles can be dispersed. For instance, the coverage of the hydrophilic silica spheres with a covalently attached layer of n-octadecanol (stearyl

alcohol) makes it possible to disperse the particles in apolar solvents such as cyclohexane [1,2]. Silane coupling agents provide new ways to modify the distance at which two particles start to interact [3].

A simple method to prepare monodisperse silica spheres, with radii ranging from 10 nm to a few μm, was reported by Stöber, Fink and Bohn (hereafter referred to as the Stöber method [4]). In their method, silica particles are formed through hydrolysis and condensation of a silicon alkoxide (tetrathoxysilane, TES, in this paper) in a mixture of water, ammonia and a lower alcohol (mostly ethanol, but in this paper methanol and propanol are used as well). The alcohol acts as a cosolvent for TES, which itself does not dissolve in water; the ammonia catalyzes both hydrolysis and condensation and provides the silica particles with a negative, stabilizing charge. Many people have prepared silica following Stöber's method and several studies have been performed to identify the factors that determine the final size and polydispersity of the particles [1,4–6]. However, these studies have produced only empirical relations.

It is only recently that several groups have tried to resolve the mechanisms behind particle formation and growth [7–12]. A generally accepted scheme has not yet emerged. To illustrate some of the apparent differences: Matsoukas and Gulari model the whole particle formation and growth process through a set of kinetic equations [9,10]. Nucleation is described as the condensation of two monomers. Subsequent growth is modeled as a *monomer addition* in which the active monomers are released through a rate limiting hydrolysis step. On the other hand, Bogush and Zukoski [7,8] model particle formation and growth as a *controlled aggregation of small subparticles* that are continuously being formed throughout the entire process. At the beginning, all the particles form aggregates; this continues until the charge of the aggregates becomes so high that collisions between the larger ones cannot take place any more. These stable particles (aggregates) continue to grow and become monodisperse by aggregation with smaller subparticles that are still being produced during the

growth. Bogush and Zukoski assume that not hydrolysis, but the condensation reactions are rate-limiting.

The main purpose of this work is to investigate in detail the relation between the particle microstructure and the particle morphology and to see to what extent the chemical microstructure is changed by the factors that influence the Stöber process. The kinetics and details of the growth mechanism are described elsewhere [12]. Factors that are of importance to the final particle size, polydispersity, shape and surface roughness are the temperature and the concentrations of all the substances in the reaction medium. Stöber et al. remarked that ammonia influenced the morphology of the particles [4]. Others also reported on a granular rough surface and less spherical shape for smaller particles as compared with larger particles (≥ 70 nm) [3,5,13,14]. It is also known from elemental analysis that silica particles prepared with Stöber's method still contain carbon and have a lower density and refractive index than amorphous silica [1,15]. The final sizes of the particles investigated by us cover the entire colloidal range and the particles are prepared with concentrations of reactants and solvents that are typically used in the preparation of dispersions of model colloids [1,4,6].

Particle radii were determined by static and dynamic light scattering, whereas additional information on the morphology was obtained with transmission electron microscopy. ^{13}C and ^{29}Si solid-state nuclear magnetic resonance (NMR) have provided quantitative information on the microstructure of pure silica and composite structures [16–22]. Only particles at the end of the reactions were characterized.

In order to bring the results into perspective, a comparison is made with a commercial colloidal silica, Ludox®, made by an inorganic route [23], and with a system prepared in a water in oil microemulsion [24,25]. The synthesis of silica particles in a microemulsion is a recent development and is reproduced here because of the resemblance to the Stöber method. The ammonia/water in cyclohexane microemulsion is formed with a non-ionic surfactant and TES is dissolved in the cyclohexane. With this system, small (≤ 20
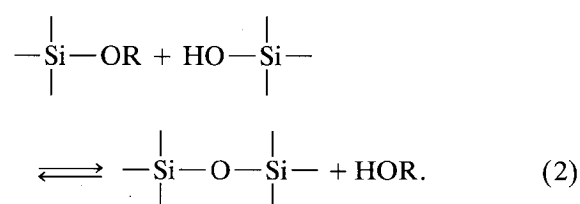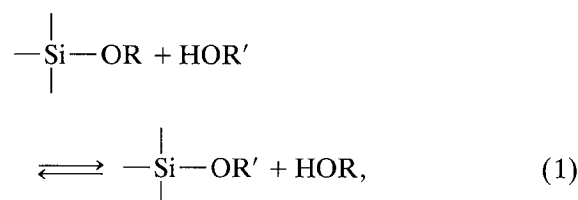
nm radius) particles can be prepared with a standard deviation in size of only a few percent.

In the next section, the chemistry of the base-catalyzed Stöber method is described and mechanistic details are given that might explain differences in the chemical structure of the particles. Also a brief background necessary to evaluate the NMR results is presented.

2. Theoretical background

2.1. Possible reactions

Alkoxysilanes in a mixture of water, ammonia, and an alcohol may undergo many different reactions. In short, these reactions can be represented as follows (other reactions not represented by eqs. (1) and (2) are assumed not to take place and only base-catalysis is considered in the following):

$$
\begin{vmatrix} \\ -\mathrm{Si-OR} + \mathrm{HOR}' \\ | \end{vmatrix}
$$

$$
\rightleftharpoons \quad -\mathrm{Si-OR}' + \mathrm{HOR}, \tag{1}
$$

$$
-\mathrm{Si-OR} + \mathrm{HO-Si-}
$$

$$
\rightleftharpoons \quad -\mathrm{Si-O-Si-} + \mathrm{HOR}. \tag{2}
$$

R and R' stand for a hydrogen atom or an alkyl group (here methyl, ethyl or propyl). The oxygen atoms bonded to silicon that are not depicted are part of a silanol group, an alkoxy group or a siloxane bond with another silicon atom.

The reactions given in eq. (1) constitute ester exchange (eg., the exchange between an ethoxy and propoxy group), hydrolysis and their reversals. It is generally believed that in the base-catalyzed case these reactions proceed through a nucleophilic attack on the silicon atom, resulting in a pentacoordinate transition state (S_N2 mecha-

nism [26–29]). Since no reaction or growth kinetics are investigated in the present paper, the effect of several reaction conditions will be described only qualitatively. Quantitative results can be found in the literature [11,28,29].

In hydrolysis, OH^- is the acting nucleophile: an increase in the concentration of this catalyst will increase the reaction rate. Thus, the rate will be increased by increasing the concentration of NH_3 and/or H_2O. Faster rates can also be obtained at higher temperatures. The role of the co-solvent is complex [11]. The nature of the groups bonded to the central silicon atom and of the leaving group also play their role in the resulting reaction rate. An increase of the positive charge on the silicon atom through electron withdrawing groups will facilitate the attack of the nucleophile. Therefore, the subsequent hydrolysis of the four alkoxy groups from a tetraalkoxysilane proceeds faster the more alkoxy groups are already removed. This increase in rate is caused by the increasing positive charge on the silicon atom and the decreasing steric hindrance of the alkoxy groups.

The leaving group has to take with it the negative charge of the transition state. It is therefore not surprising that the rate is increased if the leaving group has a better mechanism to accommodate this charge. A decrease in pK_a of the leaving groups results in an increase in reaction rate [26,27].

The condensation reactions (2) also take place through a base-catalyzed nucleophilic attack, resulting in a pentavalent transition complex. Therefore, the influence on the reaction rate of $[H_2O]$, $[NH_3]$ and the alcohol used is almost the same as for the hydrolysis [23,26,27]. The absolute rate of siloxane bond formation, however, is generally much higher than that of hydrolysis reactions of the alkoxide [30]. Possible reasons are: most silanol groups deprotonate easier than water, and tetrahydroxysilane bears a more positive charge on its silicon atom than the tetraalkoxide and possesses a better leaving group.

The attacking nucleophile for the condensation reactions is a deprotonated silanol group. The acidity of a silanol group strongly increases if the silicon atom to which it is bonded is linked

through siloxane bonds with other silicon atoms. Therefore, monomers react preferentially with higher polymerized species [23]. This reaction explains why only very high condensed species and monomers, and almost no products in between these extremes, are detected during base-catalyzed condensation of alkoxysilanes [30].

Under certain conditions, for instance high [TES] and/or low water concentrations, the reaction between partially hydrolyzed species must also be considered. In this case, the condensation and hydrolysis reactions can occur in one step: after attack of a silanolate ion, the transition state can subsequently lose an alkoxy group. Alkoxy groups that end up on a highly condensed unit are then much more difficult to hydrolyze because of steric effects [27].

2.2. ^{13}C, ^{29}Si solid-state nuclear magnetic resonance (NMR) spectroscopy

Solid-state NMR spectroscopy is a powerful method to characterize the chemical structure of substances that can be prepared from alkoxysilanes [31]. In the solid state, the line width is increased owing to dipole–dipole interactions and the anisotropy of the chemical shift tensor. Magic-angle spinning (MAS) and high-power decoupling make it possible to obtain high-resolution spectra. These techniques perform the averaging of the dipolar interactions and chemical shift anisotropy that is accomplished in a liquid by the rapid motions of the molecules in solution (with respect to the magnetic field).

By manipulation of the spins in the rotating frame, the transfer of magnetization from ^{1}H nuclei to ^{13}C or ^{29}Si nuclei becomes possible [32]. This transfer of magnetization, mainly through dipolar interactions, is called cross-polarization (CP), and leads to an increased signal intensity. Contrary to direct excitation of ^{13}Cu and ^{29}Si nuclei, the necessary delay between acquisitions is now determined by the relatively short spin–lattice relaxation time, T_{1H}, of the protons and not by the long relaxation time, T_{1C} and T_{1Si}, of the ^{13}C or ^{29}Si nuclei, which is a further advantage of CP. Because dipole–dipole interactions decay with the third power of the distance, only

those nuclei in the proximity of protons are detected. For surface-coated silica with a core consisting of pure SiO_2, this would mean a selective detection of only those nuclei close to the surface where silanol groups and other proton-containing species (water, ethoxy groups) are present.

Through siloxane bonds, a silicon atom can be bonded to a maximum of four other silicon nuclei. The number of siloxane bonds is designated by the number in the notation: Q^4, Q^3 or Q^2. The Q stands for quaternary, that is, having the ability to form four siloxane bonds. This representation originates from the old silicone polymer chemistry [33]. It is easy to differentiate between Q^4, Q^3 and Q^2 silicons, because the chemical shifts lie approximately 10 ppm apart (Q^4 at -110 ppm, Q^3 at -100 ppm, etc.). Unfortunately, the differences in chemical shifts that are caused by the exchange of a silanol group by an ethoxy group are too small to be detected in a solid-state ^{29}Si spectrum (see ref. [20] for a literature survey of the chemical shift values of Q silicons).

Maciel and co-workers showed that surface Q species of silica gels could be determined, quantitatively, by ^{29}Si MAS-CP NMR [16–18]. To obtain these quantitative results, however, it was necessary to determine T_{H-Si} and $T_{1\rho H}$ for all the different Q species.

As was stated above, CP is a selective method to excite nuclei. Q^4 silicons far away from protons are not detected with CP. It was, therefore, argued by Fyfe et al., not to use CP excitation but direct pulse excitation of the ^{29}Si nuclei to obtain quantitative results on all the silicon nuclei [19]. The delay between two pulses is now determined by the T_{1Si} of the different silicon nuclei and these relaxation parameters have to be measured first. Fyfe et al. further demonstrated with materials, similar to those described in the present paper (not fully condensed silica gels), that MAS alone was sufficient to remove the relatively small dipolar interactions and chemical shift anisotropy.

In a recent paper on the use of ^{29}Si MAS-NMR to obtain quantitative information about the siloxane structure of silica gels, Pfleiderer et al. compared the results obtained by direct pulse excitation and CP excitation [22]. They concluded

that in most cases CP excitation can provide reliable quantitative results, except for cases where dependable relative intensities including bulk Q^4 ^{29}Si are required.

As far as we know only Badley et al. [15] reported quantitative ^{29}Si results for only one batch of 'Stöber' silica particles.

Just as the ^{29}Si chemical shift for a Q species is altered very little by the exchange of a silanol group with an ethoxy group, the ^{13}C chemical shift of the carbon next to oxygen is also hardly changed if an ethanol group becomes bonded as an ethoxy group to a silicon atom [18]. In order to still be able to tell if ethoxy groups detected with CP ^{13}C NMR were bonded to silicon or not, particle synthesis was also performed in methanol and n-propanol.

3. Materials and methods

Alcosols, i.e., silica particles as dispersed in their reaction medium, are referred to in this paper as Ax, with x being a numeral. The A was replaced by a P or a M if the alcohol used was not ethanol but n-propanol or methanol respectively. Silica spheres coated with stearyl alcohol (n-octadecanol) are designated AxS.

Some of the results described here have been presented elsewhere [3]; the same particle coding will be used in the present paper. Also, some of the silica particles studied in this work have been used in earlier studies. To be able to recognize the systems, some translation is necessary. A3S is used in many investigations as SJ9 [34,35]. SM2, known here as A1, is described by Penders [36].

3.1. Materials and particle synthesis

Methanol (Baker), ethanol (Merck), n-propanol (Baker) and cyclohexane (Baker) were of analytical reagent quality. Only for the large scale (9 l) synthesis of system A1 (see table 1), absolute technical grade ethanol (Nedalco) was used. The alcohols and tetrathoxysilane (Fluka, purum grade) were freshly distilled before each synthesis. Ammonium hydroxide (Merck, 25%) was of analytical reagent quality and contained 14.0

Table 1
Reactant concentrations

System	[TES] (M)	[H$_2$O] (M)	[NH$_3$] (M)	Solvent
A1	0.155	0.855	0.318	ethanol
A2	0.0119	5.51	0.682	ethanol
A3	0.17	1.65	0.68	ethanol
A4	0.167	1.58	0.512	ethanol
A5 [a]	0.159	3.01	1.12	ethanol
A6	0.160	2.65	0.986	ethanol
A9 [b]	0.169	2.58	0.960	ethanol
A10 [c]	0.148	5.31	1.97	ethanol
M1	0.161	2.50	0.928	methanol
P1	0.178	1.03	0.383	propanol

[a] Reaction temperature 25°C.
[b] Reaction temperature 55°C.
[c] Reaction temperature 10°C, all other temperatures 20°C.

mol/l NH$_3$ as indicated by titration. The nonionic surfactant Igepal CO-520® (Aldrich) – a polydisperse preparation of polyoxyethylene nonylphenyl ether with on average five oxyethylene groups per molecule (NP-5) – was used as received. The silica, Ludox® AS40, stabilized by ammonia, was kindly provided by Du Pont.

Alcohols were synthesized according to the method of Stöber et al. [4] and the detailed description given by van Helden et al. [1]. Reaction temperature was 20°C, unless stated otherwise. The alcosol synthesized at 55°C was heated in a closed container to prevent the loss of ammonia. Preheated TES was added by injection through a septum.

Concentrations of reactants used are given in table 1; in calculating the concentrations, volume contraction was assumed to be absent. It should be emphasized that mixtures of water, ammonia and the lower alcohols show quite large volume changes at mixing. These effects depend in a non-linear, unknown way on the alcohol used and the concentration of ammonia and water. For this reason, the concentrations were calculated assuming additivity of all the liquid volumes at 20°C, using densities as given in ref. [37].

N-octadecanol coated particles were prepared as described by van Helden et al. [1].

The silica spheres made from TES in a water/ammonia in cyclohexane microemulsion were prepared as described by Arriagada and

Table 2
Radii according to transmission electron microscopy and static and dynamic light scattering (SLS and DLS)

System	TEM (σ, %) (nm)	SLS (nm)	DLS (nm)
A1	9.01 (20)		9 $\pm$2
A2	50.2 (150)		
A3S	30.9 (13)	39.6 $\pm$ 0.5	38.5 $\pm$ 0.5
A4	3‡.2 (13)	40.2 $\pm$ 0.5	36.6 $\pm$ 1.6
A5	62.4 (11)	71.5 $\pm$ 0.4	72.1 $\pm$ 1.2
A6	89.4 (6)	107.2 $\pm$ 0.3	108.1 $\pm$ 0.7
A9	75.2 [a] (21)		
A10	481	506 $\pm$4	
M1	18.2 (16)	26.1 $\pm$ 0.9	30 $\pm$2
P1	24.2 (12)	33.1 $\pm$ 0.5	35.1 $\pm$ 1.3
Ludox	11.1 (20)	17.5 $\pm$ 0.3	20.8 $\pm$ 0.5
μE1	23.5 (3.5)		

[a] Also visible were open, irregular flocculates ($\approx$ 100 nm) of $\approx$ 10 nm irregular particles.

Osseo-Asare [25] with $[H_2O]/[NP-5] = 1.9$ (their 'R' value). In 800 ml cyclohexane, 41.0 ml NP-5 was dissolved under slow stirring. Subsequently, 4.85 ml ammonia and 30 min later 5.00 ml TES were added. During the whole reaction time of 7 days, the reaction mixture was slowly stirred at 20°C. This silica system is further referred to as μE1.

3.2. Light scattering

Light scattering measurements were made at 25.0 $\pm$ 0.1°C using very dilute dispersions in ethanol.

Static light scattering (SLS) was performed with a Fica-50 photometer using vertically polarized incident and detected light ($\lambda = 436$ and 546 nm). A correction was made for scattering of the solvent. Mean intensities as a function of the scattering angle were obtained in the range 20° $\leq$ $\theta \leq 150°$. An optical radius (table 2) was obtained from an analysis of the intraparticle interference in the Rayleigh–Gans–Debye approximation as described in refs. [1,38]. The particles of A10 were analyzed using Mie scattering theory [39]. No irregularities at low scattering angles were observed, indicating dust free, non-clustered sols.

Dynamic light scattering (DLS) results were obtained using an argon ion laser (Spectra Physics Series 2000). Auto correlation functions were measured with a Malvern Multibit K7025 128 points correlator. Diffusion coefficients were obtained from a second order cumulant fit [40] using auto correlation functions obtained from six scattering angles between 35 and 145°. Except for dispersion A1, the normalized second cumulant yielded values ≤ 0.05; the value for A1 was ~ 0.12. A hydrodynamic radius (table 2) was calculated using the Stokes–Einstein relation:

$$D_0 = \frac{k_B T}{6\pi\eta R_h},\qquad(3)$$

where k_B is Boltzmann's constant, T is the absolute temperature, η is the solvent viscosity and R_h is the hydrodynamic radius.

More general information about SLS and DLS can be found in refs. [39,41].

3.3. Electron microscopy

Transmission electron micrographs were made by dipping copper 400 mesh carrier grids in a dilute dispersion. The grids were covered with carbon coated Formvar films and the photographs were made of particles retained on the film. Philips EM301 and Philips CM10 transmission electron microscopes were used, with the magnification calibrated with a diffraction grating.

Particle radii of 200–2000 particles were measured using an interactive image analysis system (IBAS). Assuming a spherical shape, the surface area of the particles was used to determine a number averaged particle radius, $\langle R \rangle$, and the relative standard deviation, σ, as defined in

$$\sigma^2 = \frac{\langle R^2 \rangle - \langle R \rangle^2}{\langle R \rangle^2}.\qquad(4)$$

3.4. NMR spectroscopy

High-resolution solid-state NMR spectra were measured at room temperature on a Bruker AM 500 spectrometer (silicon frequency 99.4 MHz,

carbon 125.7 MHz) equipped with a Bruker solid-state accessory. Spectra were obtained using a broadband probehead with a 7 mm double air bearing magic-angle spinning assembly. Spinning speeds ~ 4000 Hz were employed. The 90° pulse lengths for the nuclei ^{13}C, ^{29}Si and ^{1}H were ~ 5.5 μs. Cross-polarization (CP) contact times lay between 0.5 and 4 ms for carbon and 0.5 and 6 ms for silicon; phase cycling and spin temperature alternation were used to minimize artifacts. The delay time between pulses in the CP experiments was 4 s. The number of accumulated FIDs for CP spectra ranged between 200 and 4000, depending on the system being investigated.

Adamantane and the trimethylsilyl ester of double four-ring octameric silicate, Q_8M_8, were used to optimize experimental parameters and as external secondary chemical shift reference relative to tetramethylsilane for ^{13}C and ^{29}Si respectively. Chemical shift values are given in parts per million.

Some of the samples used for NMR were freeze-dried to prevent any reaction during the drying process; others were dried under nitrogen at 90°C for 24 h. P1, A6 and μE1 were also washed three times with deionized water after centrifugation of the dispersion. The washings were used to determine if the alkoxy groups that were detected were only present on the particle surface. Typically, the spinner was filled with 300 mg silica.

A determination of silicon relaxation times, T_{1Si}, with direct excitation was not considered practical after a first estimation of these values. Instead, CP excitation was chosen according to the method described by Torchia [42] using contact times of 4 ms.

Based on the longest T_{1Si} values, a delay time of 300 s between successive direct ^{29}Si excitations was chosen for the quantitative determinations of the siloxane structure. Typically, 250 FIDs were accumulated.

Deconvolution of the spectra was performed by adjusting the height, width and frequency of Gaussian lineshapes to obtain the best visual fit. This was done manually using the Bruker program Glinfit or automatically using NMR, again using Gaussian lineshapes.

Table 3
Elemental analysis (weight percentages) [a] and particle density, ρ

System	C (%)	H (%)	ρ (g/ml)
A1	1.11 ± 0.02	0.99 ± 0.08	
A2	0.59 ± 0.01	0.85 ± 0.02	
A3S [b]	9.7	2.7	
A4			1.99
A5	5.07 ± 0.12	1.66 ± 0.07	1.98
A6	3.95 ± 0.04	1.55 ± 0.08	2.03
A6 [c]	3.54 ± 0.03	1.45 ± 0.08	
P1	3.84 ± 0.02	1.55 ± 0.04	
P1 [c]	0.27 ± 0.04	1.34 ± 0.10	
A10			2.03
Ludox			2.20 [d]

[a] Errors indicate differences in duplicate results.
[b] Silicon percentage 39.0% [34,35].
[c] Samples were washed for three hours with water before drying.
[d] Ref. [23].

3.5. Elemental analysis and particle density

Elemental analysis was carried out by Elemental Microanalysis Limited (Devon, UK). Prior to sending, the samples were dried during 24 h at 100°C under nitrogen. Before the measurements were made they were dried again for 3 h under the same conditions.

Particle densities were determined by drying a known volume of a concentrated dispersion in ethanol under dry nitrogen at 100°C for 24 h and weighing the residue. The densities of A4, A5, A6 and A10 were measured (see table 3).

4. Results

4.1. Particle size and morphology

All the alcohols with a relatively small standard deviation were investigated with SLS and DLS; the determined radii are given in table 2. No indication of clustering was found. However, after a few weeks, the methanosol flocculated. The other systems remained stable. For the alcosol A10, it was important to reduce the concentration of ammonia four times directly after the synthesis by dilution with ethanol, to obtain a sol

stable for a long time (see also ref. [12]). A10 was the only system where the Mie scattering theory had to be used to analyze the SLS. DLS on this system was very difficult because of the rapid decrease in intensity with scattering angle.

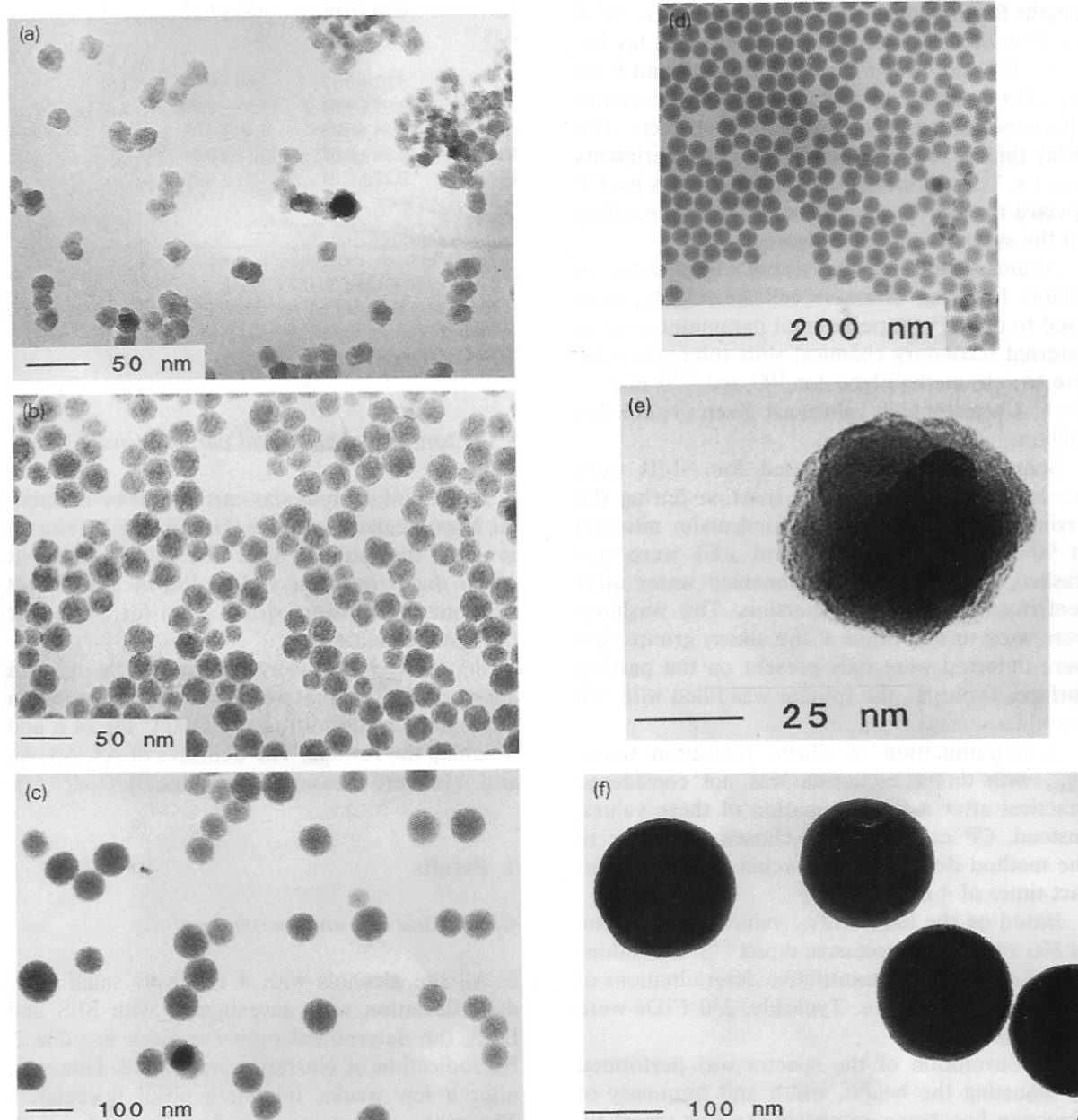Number-averaged, mean radii and relative

Fig. 1. Transmission electron micrographs. (a) A1 $\langle R \rangle = 9.01$ nm (20%), supercritically dried. (b) Ludox $\langle R \rangle = 11.1$ nm (20%). (c) A2 $\langle R \rangle = 50.2$ nm (150%). (d) μE1 $\langle R \rangle = 23.5$ nm (3.5%). (e) A4 $\langle R \rangle = 31.2$ nm (13%), supercritically dried. (f) A6 $\langle R \rangle = 89.4$ nm (7%).

standard deviations as determined with transmission electron microscopy are given in table 2. Typical particle morphologies are shown in fig. 1. The rough surface and not perfect spherical form as found in figs. 1a (A1) and (e) (A4) was also seen for the systems A3S, M1 and P1. The Ludox® particles (fig. 1(b)) are already more spherical

and less rough, but are still irregular compared with the smooth, perfectly spherical particles shown in figs. 1(c) (A2) and (d) (μE1). (The seemingly hexagonal shape of the particles in fig. 1(d) is an optical illusion caused by the regular packing and disappears if one only focuses on single particles.) Besides its perfect shape, the
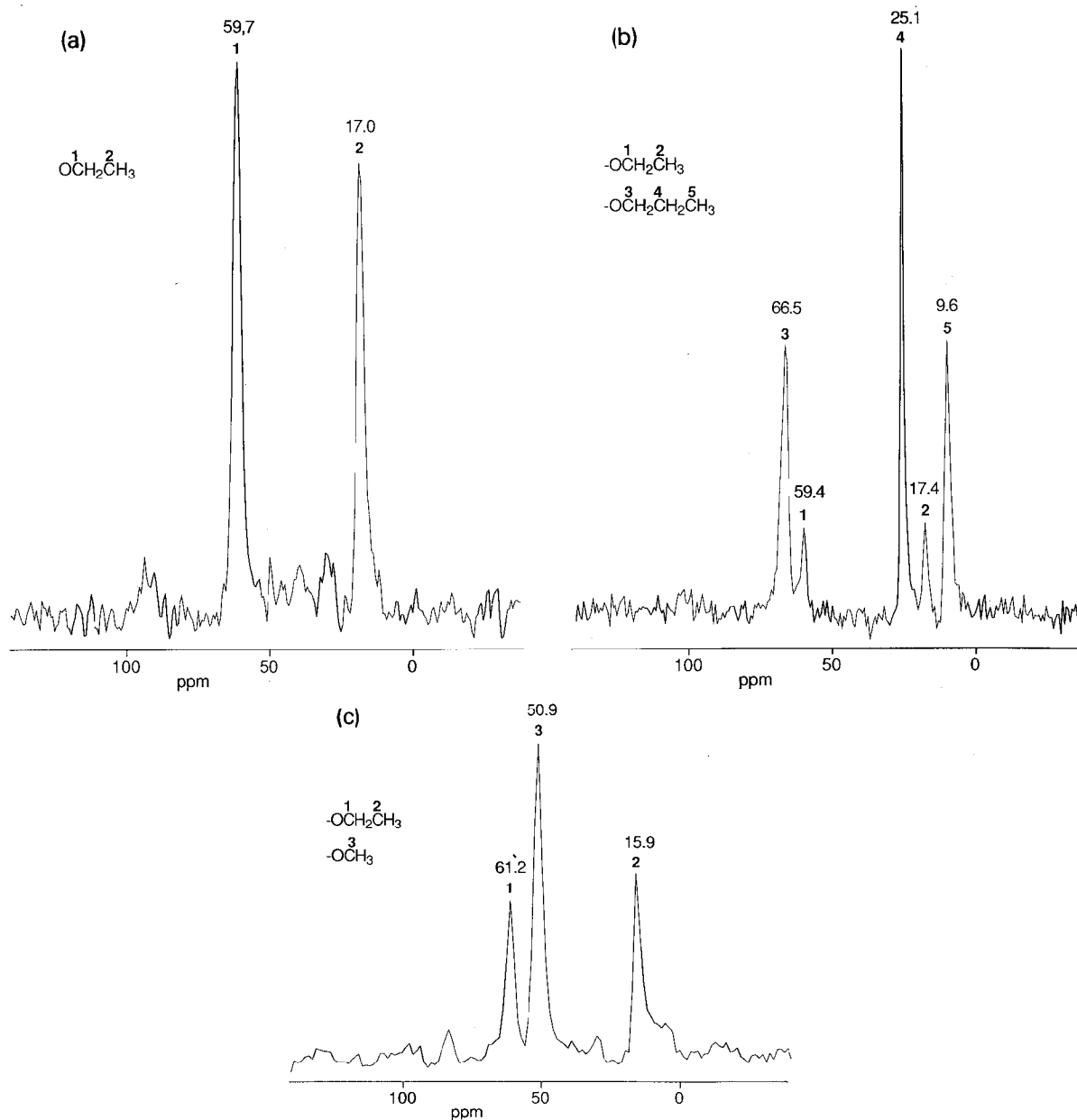

Fig. 2. ^{13}C CP-MAS NMR spectra of alkoxy groups in silica, mixing time 1 ms. (a) A1, 1000 accumulations. (b) P1, 500 accumulations. (c) M1, 3000 accumulations.

particles prepared in the microemulsion are also extremely monodisperse considering their size. For the 'normal' Stöber process with TES concentrations around 0.17M, these types of perfect sphere are only formed if the final particle radius is larger than ≈ 70 nm (see fig. 1(f) (A6) and ref. [2]). A monodispersity comparable to that of μE1 is only reached for particles with radii larger than ≈ 150 nm.

4.2. NMR spectroscopy

4.2.1. ^{13}C spectra

^{13}C CP-MAS NMR showed the presence of ethoxy groups in all the silica particles prepared in ethanol (fig. 2(a)). The carbon of the methyl group was found close to 17 ppm and the carbon bonded to oxygen had a chemical shift around 59 ppm. It is possible that the CP parameters differ

for different samples. However, there is qualitative agreement between the intensities of the CP ^{13}C carbons (relative to the noise level) determined with contact times of 4 ms and the elemental analysis results given in table 3. This indicates that the CP efficiency does not differ too much between different samples with mixing times of 4 ms.

To determine to what extent the ethoxy groups `would` be removed by hydrolysis, some samples `were` washed several times with water. Again the the elemental analysis results were in agreement with the disappearance of the carbon signal after the water washing of P1 and the small change of the signal of A6 after the same treatment (see table 3 and the experimental section on NMR). The presence of ethoxy groups in the spectra of A3S and μE1 is also eminent through the presence of the methyl group carbons at 17 ppm (figs.
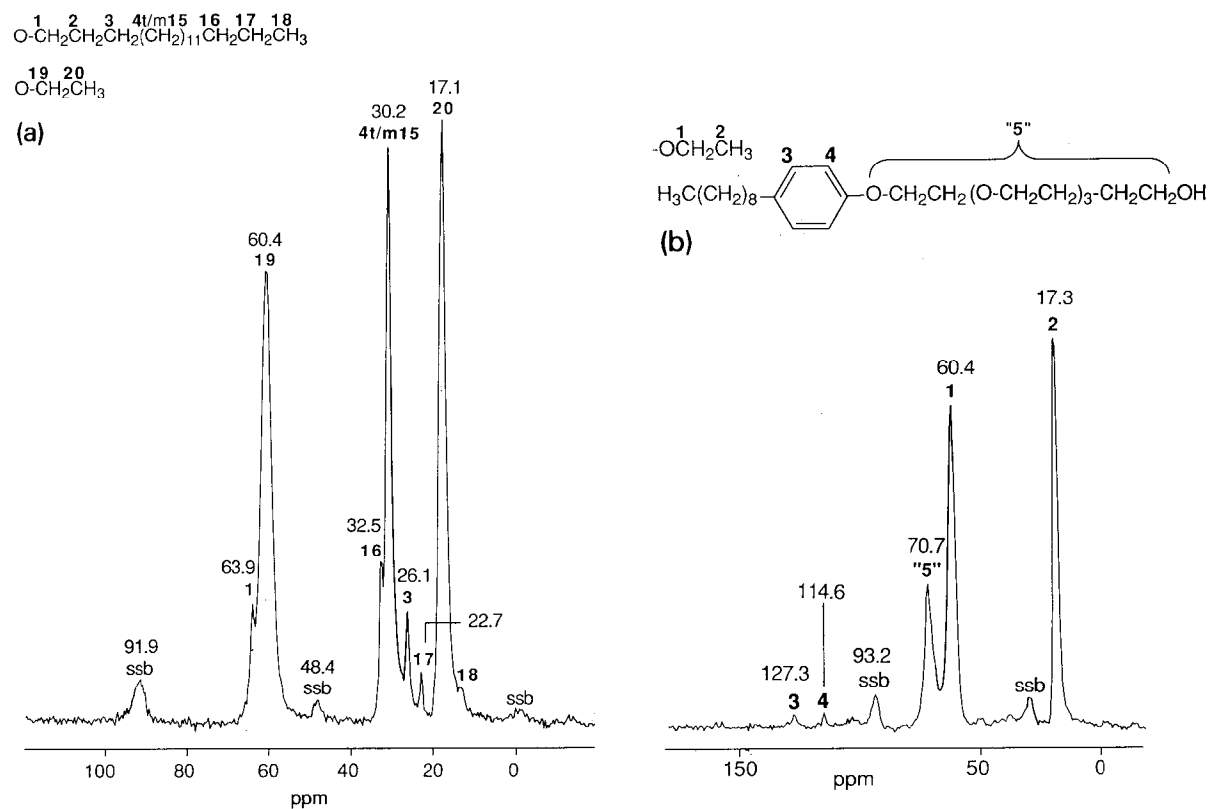

Fig. 3. CP-MAS ^{13}C spectra and shift assignments of silica samples. (a) A3S octadecanol coated (contact time 1 ms, number of scans 8000). (b) μE1 (contact time 1 ms, number of scans 13000).

3(a), (b)). These carbon signals can only be caused by ethoxy groups. As expected, fig. 3 also contains the signals of octadecyl groups and, despite the washing procedure, the polyoxyethylene nonylphenyl ether. The peak assignments of these substances were made with literature values (e.g. ref. [21]).

The chemical shifts of a carbon attached to an –OH group or an –OSi moiety are very close together [17]. Therefore, it is difficult to distinguish between ethoxy groups chemically bound and ethanol molecules bonded through hydrogen bonds with silanol groups. Further, since the particles have been prepared in the solvent ethanol, re-esterification of silanol cannot be excluded either.

In order to determine the origin of the observed ethoxy groups, the following experiments were undertaken. Instead of synthesizing silica particle in the solvent ethanol, in which the exchange of an ethoxy group from a TES molecule with a solvent molecule (also an ethoxy group) cannot be proven, particles were also synthesized

in methanol and n-propanol. Now the exchange between an ethoxy group and a methoxy or propoxy group could be observed without difficulties. All alkoxy groups are present in the spectra in figs. 2(b) and 2(c): ethoxy groups from TES and methoxy and propoxy groups from the solvent.

4.2.2. ^{29}Si spectra

Excitation by cross-polarization was not used for a quantitative analysis, because the CP parameters differed substantially for different samples and because some of the Q^4 nuclei could not be detected by this method. These reasons are illustrated by the CP spectra of Ludox and A1 in fig. 4; the spectra were obtained with the same contact time of 4 ms. The variations in the CP behaviour is discussed more fully in section 5.2.2.

Therefore, the relaxation times of the silicon nuclei had to be estimated in order to use direct excitation to obtain the quantitative ^{29}Si spectra. High-power proton decoupling was not necessary to obtain these spectra. Even at the high mag-
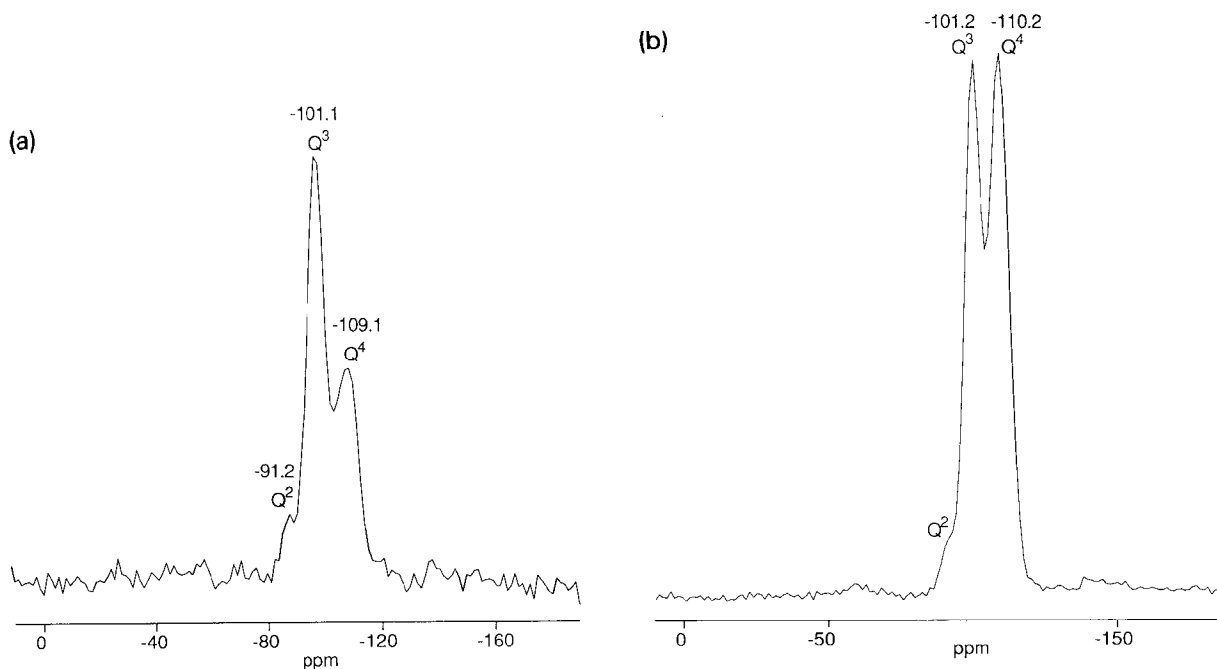

Fig. 4. CP-MAS ^{29}Si spectra of silica samples. (a) Ludox (contact time 4 ms, number of scans 2000). (b) A1 (contact time 4 ms, 2700 scans).
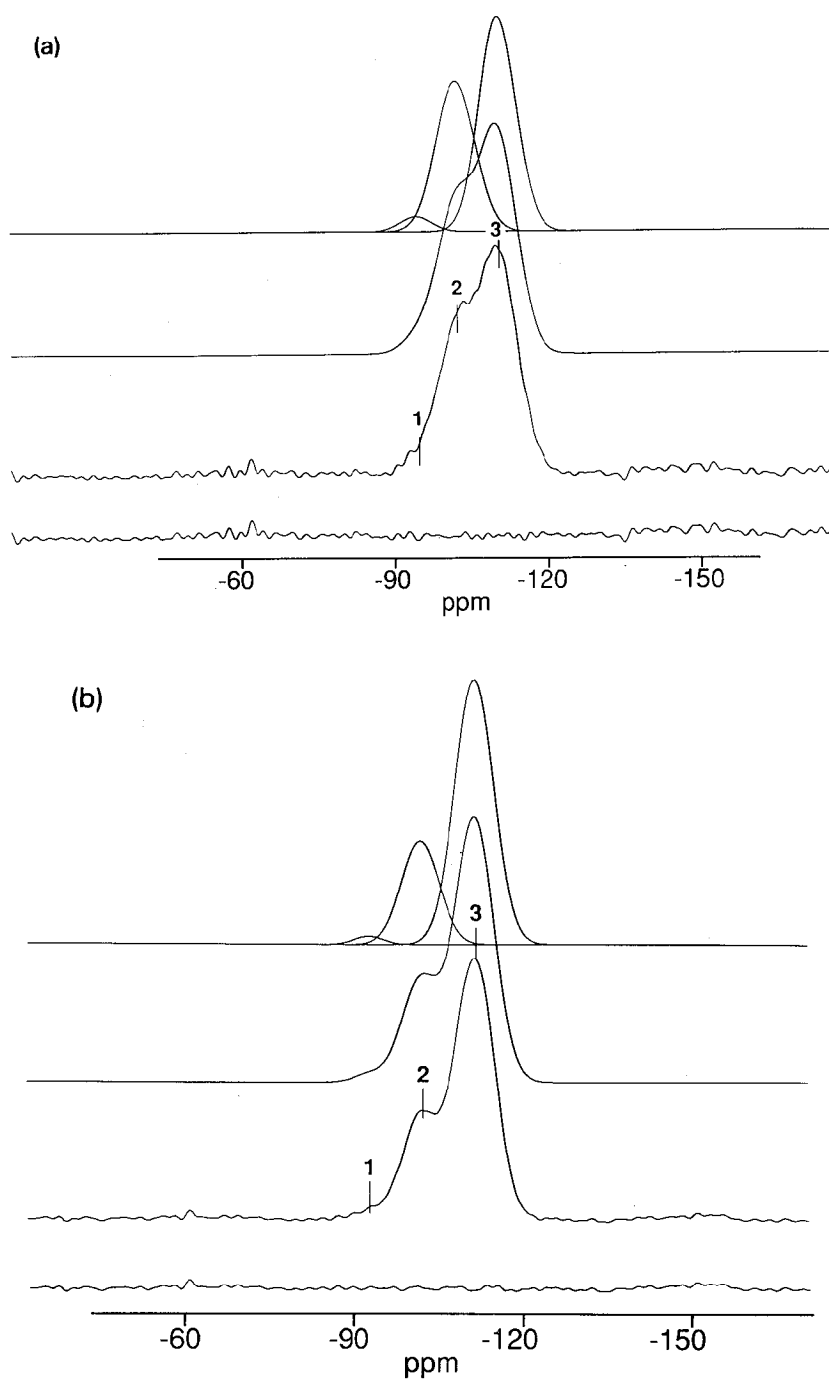
(a)

-60   -90   -120   -150
              ppm

(b)

-60   -90   -120   -150
              ppm

Fig. 5. Quantitative direct excitation ^{29}Si spectra together with Gaussian lines. (a) μE1 (delay between pulses 300 s, 224 scans): 1, -94 ppm (Q^2); 2, -102 ppm (Q^3); 3, -110 ppm (Q^4). (b) A10 (delay between pulses 300 s, 190 scans): 1, -93 ppm (Q^2); 2, -102 ppm (Q^3); 3, -111 ppm (Q^4).

netic field used, the relatively small chemical shift anisotropy and dipolar coupling with protons could be removed completely by MAS alone. This was also reported by Fyfe et al. for not-fully-hydrolyzed silica gels (see the spectra in ref. [19]).

For practical reasons the spin–lattice relaxation times of the different silicon atoms were determined using CP excitation. It is clear that a spin–lattice relaxation time obtained in this way is only an indication. For instance, quaternary silicon atoms with no, one or two silanol silicons as direct neighbours will not only have different CP parameters, but will also have different relaxation paths and will thus have differing T_{1Si} values. These differences were, indeed, observed experimentally: spin–lattice relaxation times for A1 determined with a contact time of 1 ms were < 30 s, while contact times of 4 ms indicated much longer spin–relaxation times. The curves of the logarithm of the integrated intensity vs. time were convex, implying a range of relaxation times. An estimate of the longest relaxation times gave, for Q^3 and Q^4, 55 and 85 s, respectively. The fraction of Q^4 silicons having much longer T_{1Si} values is probably small, because no differences were observed in spectra obtained with pulse delays of 300 and 400 s.

The quantitative direct excitation results obtained with delay times of 300 s are presented in table 4. Two examples are shown in fig. 5.

Table 4
Relative intensities of silicon environments

System	Q^4	Q^3	Q^2
A1	73 [a]	26	1.7
A2	69	32	–
A3S	65	31	4.1
A5	64	31	5.5
A6	66	30	4.2
A9	67	33	–
A10	71	27	1.7
M1	64	30	6.5
P1	66	28	5.6
P1 [b]	67	27	6.0
Ludox	85	15	–
μE1	55	41	3.3

[a] Estimated errors for O^4 and O^3: $+2$; for the other species ± 1.
[b] After washing procedure with water.

4.3. Elemental analysis and particle density

The elemental analysis data are presented in table 3 and the drying/weighing procedure as described in the experimental section resulted in densities that are given in table 3.

5. Discussion

5.1. Particle size and morphology

The experimental radii determined with SLS and DLS are, for most particles, similar. Differences in the radii found with SLS and DLS can be caused by differences in the underlying physical processes used to determine the radius, or by polydispersity.

A hydrodynamic radius as determined from the diffusion coefficient with the Stokes–Einstein relation (eq. (3)) of an exactly monodisperse system is expected to be somewhat larger than the optical radius that results from intraparticle interferences, because the solvent molecules, dragged along with the particle surface, can increase the radius somewhat.

Because the two radii as determined with light scattering depend on different particle properties, the mean radii that are determined for a polydisperse system are not equal. The different moments of the particle size distribution function that are measured with SLS and DLS can be found in refs. [40,43]. The result is that the mean radius as determined with SLS is larger than that determined with DLS. However, for polydispersities close to 10% (eq. (4)) the calculated theoretical differences are only a few percent, as observed in most cases (table 2).

The theoretical differences between the number averages obtained with TEM and the averages as obtained with light scattering are too small to explain the experimental differences in mean radii as obtained with these techniques [1,40]. The shrinkage and/or deformation of the particles was not caused by drying forces [2]. The electron beam intensity may be the cause of the shrinkage. The same explanation has been put forward many times and is, in view of the relative

low density of this type of silica, not unreasonable.

5.2. NMR spectroscopy

5.2.1. ^{13}C spectra and origin of carbon content

Carbon spectra are not suited to distinguish between 'free' or bonded alkoxy groups in the silica particles, because of small chemical shift differences. However, with elemental analysis alone, important information is not obtained: clear examples are the presence of ethoxy groups in the stearyl coated particles A3S and the pressence of the non-ionic surfactant after washings of μE1.

One other example is the presence of ethoxy inside the silica spheres synthesized in methanol or propanol (fig. 2). Synthesized in different solvents, the ethoxy groups can only be explained by assuming that these groups were bonded to partially hydrolyzed TES molecules. Re-esterification with already hydrolyzed ethanol is unlikely, because of the very low concentration of ethanol in the solvents methanol and propanol. Taken together with the the quantitative elemental analysis data, this analysis implies that several percent of the ethoxy groups never left the TES molecules. Further, it can be concluded from the absence of a relation between the carbon content and the particle radius and the results for the washing of A6, that most of the ethoxy groups found in the larger silica spheres are buried inside the particle and cannot be reached from the outside by the hydrolyzing water molecules. The presence of methoxy and propoxy groups (see figs. 2(b), (c)) indicates that it is likely that some re-esterification and/or ester exchange with the solvent also take place.

5.2.2. ^{29}Si spectra and siloxane structure

It has been reported in the literature that the different Q silicon atoms have different CP parameters, $T_{1\rho H}$ and T_{HSi} [16,21,22]. T_{H-Si} is due to the rate of transfer of magnetization from ^1H nuclei by dipolar interactions to ^{29}Si and $T_{1\rho H}$ is the relaxation time of the spin–locked protons in the rotating frame. The range in CP parameters is caused, mainly, by differences in the dipolar

interaction with protons. Clearly, the dipole–dipole interactions between protons and silicon nuclei are stronger for Q^2 silicons than for Q^4 silicons. The inefficient CP of Q^4 is illustrated in fig. 4(a). Although the number of Q^4 nuclei in the Ludox particles is much larger than the number of Q^2 and Q^3 nuclei (see table 4), the peak intensity of Q^3 is higher than that of Q^4 in the CP spectrum obtained with a contact time of 4 ms (fig. 4(a)). The differences in the CP behaviour of the different Q silicon nuclei suggest that there could be differences in CP parameters for a Q^x species belonging to different silica samples. An example can be found in the CP spectrum of A1 that was also obtained with a CP contact time of 4 ms (fig. 4(b)). Although the number of Q^4 silicons in this sample is smaller than in the Ludox silica (table 4), the intensity of the Q^4 peak is about equal to that of Q^3. Thus, Q^4 silicons in the system A1 are much easier to excite by CP than the Q^4 silicons in the Ludox silica. Almost certainly this is due to the local proton density which is higher in A1 than in the Ludox silica. Further, these results make it likely that even in one sample such as A1 $T_{1\rho H}$ and T_{HSi} will differ for different Q^4 silicon atoms as has been reported by Pfleiderer et al. [22]; a Q^4 atom bonded to Q^2 silicon atom will be easier to cross-polarize than a Q^4 surrounded by four other fully condensed Q^4 silicon nuclei.

Given these results, we conclude that quantitative measurements using CP can only be obtained if, for every sample, all the relaxation and polarization parameters are known. Even then, Q^4 may be underestimated, because some condensed silicon nuclei might not give a CP signal. Therefore, direct excitations were used to obtain quantitative reliable results on the relative intensities of the different Q-species.

All the observed differences in CP and relaxation parameters, even for the same Q^x silicons, indicate that these silica samples are inhomogeneous with respect to length scales and timescales that are of importance to solid-state NMR. These inhomogeneities are probably caused by differences in local proton densities, as mentioned above (number of silanol groups, ethoxy groups and water content), and differences in all dy-

namic processes (proton exchange, mobilities of ethoxy groups, physically adsorbed water and siloxane structures).

In the following sections, the differences in the siloxane structures of Ludox silica, 'Stöber' silica and the silica particles prepared in the microemulsion are discussed (see the examples in fig. 5).

From table 4 it follows that only the Ludox silica can be considered a fully condensed SiO_2 structure, with (Q^2 and) Q^3 moieties predominantly at particle surfaces. The surface and volume of the spheres can be calculated easily from the radius obtained by TEM (11 nm or light scattering, 19 nm). Assuming 4.5 OH groups per nm^2 [23], the expected number of silanol groups as a percentage of the number of silicon atoms per particle can be determined. The number of silicon atoms in a sphere can be obtained from the density (2.2 g/ml [23]) and the molecular weight, which is, taking the 15% Q^3 into account, 61.43 g/mol. These calculations result in 5.7% silanol groups using the TEM radius or 3.3% using the light scattering radius. These values are small compared with the experimental number of 15% obtained by NMR (table 4). Surface roughness, observed by TEM, will significantly increase the measured surface area. Finally, some silanol groups inside the particles cannot be excluded, even for these condensed structures.

From the calculations for the Ludox silica particles and the results of tables 2 and 4, it is clear that the high Q^3 and Q^2 content of the 'Stöber' particles cannot be explained only by silanol groups on the surface of the spheres. The smallness of the changes in the siloxane structures of these silica systems is remarkable, despite apparent differences in radius, carbon content (table 3) and reaction temperature during the synthesis. Even the heating for several hours at 200°C during coating with octadecanol did not change the siloxane structure of A3S significantly.

To our knowledge, there is only one study in which a quantitative ^{29}Si NMR result of 'Stöber' silica has been reported [15]. In this study on the coating of silica particles, Badley et al. measured only the Q intensities of one silica system. The radius of the particle measured by TEM was 29

nm and the quantitative results found were: 4% $\pm$ 1% Q^2, 38% $\pm$ 2% Q^3 and 58% $\pm$ 2% Q^4. These intensities were obtained with direct excitation and a pulse delay of 150 s. The reported values of T_{1Si} ranged from 30 to 40 s. Probably, the low Q^4 content as compared with the values obtained in this work is caused by an underestimation of the relaxation times of some of the Q^4 silicons.

Surprisingly, the siloxane structure of the silica prepared in the microemulsion is significantly less condensed than all the other silica particles studied. The number of Q^3 and Q^2 nuclei is almost as large as the number of Q^4 silicons. Explanations for the hindered condensation of TES in this system clearly need further study.

5.3. Particle composition and density

The results of elemental analysis as given in table 3 can be used together with the relative intensities of Q species to calculate the number of alkoxy groups per silicon. The NMR result on the siloxane structure are needed, because, except for A3S, no elemental analysis was done for silicon and oxygen. The fraction in the elements silicon and oxygen 1 g of silica is obtained by subtracting from 1 g the weight of hydrogen and carbon as given in table 3. For pure silica (SiO_2), this quantity can be converted to n moles of silica, using the molecular weight 60.08 g/cm^3. However the silicas studied do not consist of pure $nSiO_2$, but of $nSiO_x$. The x can be calculated using the relative Q intensities from table 4. For example, if a silica contains only Q^2 silicon nuclei, the x would be 3, because in this siloxane structure there are three oxygen atoms for every silicon atom. In this way, the number of moles TES that were incorporated in 1 g of (dried) silica can be calculated and compared with the number of ethoxy groups calculated from the carbon percentage. The number of ethoxy groups as compared with the number of silicon atoms ranges from a few to 14% for sample A5.

No elemental analysis was performed on the silica μE1 because it was contaminated by the non-ionic surfactant (see fig. 3(b)). Thus, no quantitative percentage of ethoxy groups could be

calculated. The quite strong CP ^{13}C signals of the ethoxy groups imply, however, that a substantial amount of OC_2H_5 must be present inside the particles.

A check for consistency of the data can be made by using the $nSiO_x$ structure and carbon data to calculate the weight percentage of hydrogen (table 3). In this calculation, it is assumed that all ethoxy groups are bonded with a silicon atom and are not present as ethanol (see the ^{13}C NMR results). In all cases a reasonable agreement is found; mostly an amount of only 0.1 or 0.2% is not accounted for. This means that it is not clear if the above-mentioned assumption about the bonding of the ethoxy groups is correct; however, it can be concluded that not much physically adsorbed water is present.

For the sample A3S, the amount of silicon was also determined: 39.0% (elemental analysis described in refs. [34,35]). Subtracting C and H and using the siloxane structures from NMR as before, one obtains 38.9% Si. This agreement implies that physically absorbed water is absent in this particle. This result is not strange considering the reaction temperature of 200°C necessary for the three hours during esterification. Jansen and co-workers [34,35] reported that A3S contained 5% water; this value was calculated assuming a pure SiO_2 siloxane structure. Because of the NMR results, it is clear that the OH groups are not present as physical bonded water, but as chemically bonded silanol groups.

The combined results of carbon NMR and elemental analysis make it very probable that, for most reaction conditions, at least several percent of the ethoxy groups never leave the TES molecules. This finding is in agreement with kinetic studies in which it is shown that hydrolysis is the rate limiting step [9,10,12].

The densities obtained in this work (between 1.98 and 2.03 g/cm^3 (table 3) are in good agreement with the values obtained by Badley et al. (their densities were between 2.06 g/cm^3 for a particle with a 30 nm radius and 2.02 g/cm^3 for a particle with radius 325 nm [15]), and Bogush et al. (2.04 to 2.10 g/cm^3 [6]). The disappearance of the alkoxy groups of P1 after washing with water (see the ^{13}C results) indicates a (micro) porosity

also proposed by van Helden et al. [1]. Together with the siloxane structure, this porosity explains the low density of 'Stöber' silica compared with amorphous bulk silica and Ludox silica (2.2 g/cm^3 [23]). For the larger particle, A6, the porosity is not sufficient to hydrolyze most of the ethoxy groups in the interior of the particle.

5.4. Particle growth mechanism

The dependence of the final particle radius on reaction conditions follows the same general trends described before [1,5,6]: the particle radius increases with increasing concentration of water and ammonia for relative low concentrations of these reactants. Explanations for these dependencies are provided in a paper in which the dynamics and mechanism of particle formation and growth are discussed [12]. Larger particles are also formed at lower temperatures. The improvement in particle shape and surface roughness with increasing radius is clearly visible (fig. 1 and ref. [13]).

Small particles synthesized at high water and low TES concentrations A2 (fig. 1(c)) and the even smaller particles obtained in a microemulsion, μE1 (fig. 1(d)) do not follow the trends in final particle shape and radius. Although being small, these particles have a smooth, spherical shape compared with particles synthesized from TES concentrations close to 0.17M according to Stöber. We expect to see effects on the particle morphology if the chemical silica structure of the particles is less regular because of silanol groups and ethoxy groups inside the spheres. However, the chemical microstructure as determined with NMR and elemental analysis indicate that, for these particles, morphology is not a function of chemical structures that are the building units of these particles: the low ethoxy content of A2 is as expected (see section 2), given the high water and low TES concentration used. A condensed structure such as the Ludox silica, however, did not result from this low carbon content. Thus, the spherical shape is not a direct result of a highly condensed siloxane structure. This is indicated by the very low Q^4 to Q^3 ratio of μE1 as well. For this system, the spherical shape is also accompa-

nied by a high content of ethoxy groups, which again indicates that the chemical microstructure does not affect particle morphology.

Since the different particle morphologies do not correlate with the chemical structure of the particles, we propose, instead, that the observed differences in particle form and surface roughness are caused by a difference in the molecular weight of the building silicon moieties reacting with the growing particle. This conclusion is also confirmed by kinetic measurements [12]. Early in the reaction, the condensing units causing the particle to grow consist of larger silica structures ($\approx$ nm or larger). For the conditions at which smaller final particles are formed – for TES concentrations around 0.17M (see table 1) – the growth by larger structures continues throughout most of the reaction period. This type of growth results in irregularly shaped particles with rough surfaces. For the particles formed in higher water and ammonia concentrations, we propose that the later stages in the growth are by the condensation of monomers or small oligomers on the surface. In this way a smooth, spherical particle shape is achieved. The siloxane microstructure of both the regular and irregular shaped particles is determined by the condensation mechanism of reacting TES or (partially) hydrolyzed TES molecules with the particle surface and/or substructures.

Also, with the particles produced at low TES concentrations such as A2 and very probably also in the case of μE1, a monomer addition is responsible for the morphology. Aggregation of subparticles for the growth of μE1 as proposed in ref. [23] is unlikely in view of the particle form which is smooth and spherical even early in the reaction. However, conclusions about the mechanism of particle growth in a microemulsion are speculative; the non-ionic surfactant polyoxyethylene nonylphenyl may end up inside the particles. The shape and very low polydispersity certainly warrant a more systematic study of these mechanisms.

The conclusions about the difference in size of the structures that condense on a particle surface are confirmed by recent cryogenic transmission electron microscopy results of Bailey and Mecart-

ney [14]. They looked at vitrified reaction mixtures early in the reaction. In propanol as solvent, they first observed low density, polymer-like structures of 26 nm. These structures seemed to collapse into high density particles with an average size of 20 nm having a rough texture. No small, high density subparticles were seen during the growth to a final size of 200 nm. They also propose a growth at later stages in the reaction mainly through the addition of monomers and/or very small low density substructures that are not visible with TEM.

6. Conclusions

The experimental results make it quite clear that quantitatively reliable results about all the Q species, including Q^4, can only be obtained with direct excitation of the silicon nuclei. For quantitative CP, it would be necessary to determine fully the spin dynamics for each sample, and, even then, some Q^4 species would possibly not be detected. However, it is still important to determine the spin–lattice relaxation times of samples containing the most Q^4. If CP excitation is used in the determination of T_{1Si}, the silicons with the longest relaxation times might not be excited resulting in an underestimation of the relaxation times. The necessity to be careful even if using direct excitation is illustrated by the results obtained by Badley et al. [15].

Contrary to Ludox silica particles, 'Stöber' silica particles are not fully condensed and contain around 60% Q^4, 30% Q^3 and several percent Q^2. The differences in the siloxane structure that were found in this study were small for particles prepared following the method of Stöber. The radii and shape and surface roughness of the particles varied significantly.

Several percent of the ethoxy groups of the TES monomers are never hydrolyzed and end up inside the particles. Particles synthesized in higher water concentrations or the smaller particles after washing with water contain less ethoxy groups. These findings are not accompanied with a substantial increase in Q^4.

References

[1] A.K. van Helden, J.W. Jansen and A. Vrij, J. Colloid Interf. Sci. 81 (1981) 354.

[2] A.K. van Helden and A. Vrij, J. Colloid Interf. Sci. 78 (1980) 312.

[3] A. van Blaaderen and A. Vrij, 'Synthesis and characterization of colloidal model particles made from (organo)-alkoxysilanes', paper presented at R.K. Iler Memorial Symposium, Washington, Aug. 1990, to appear in Advances in Chemistry, Series No. 234, Colloid Chemistry of Silica, ed. H. Bergna, in press.

[4] W. Stöber, A. Fink and E. Bohn, J. Colloid Interf. Sci. 26 (1968) 62.

[5] H. Giesche, PhD dissertation, Johannes Gutenberg Universität Mainz (1987).

[6] G.H. Bogush, M.A. Tracy and C.F. Zukoski IV, J. Non-Cryst. Solids 104 (1988) 95.

[7] G.H. Bogush and C.F. Zukoski IV, J. Colloid Interf. Sci. 142 (1990) 1.

[8] G.H. Bogush and C.F. Zukoski IV, J. Colloid Interf. Sci. 142 (1990) 18.

[9] T. Matsoukas and E. Gulari, J. Colloid Interf. Sci. 124 (1988) 252.

[10] T. Matsoukas and E. Gulari, J. Colloid Interf. Sci. 132 (1989) 13.

[11] M.T. Harris, R.R. Brunson and C.H. Byers, J. Non-Cryst. Solids 121 (1990) 397.

[12] A. van Blaaderen, J. van Geest and A. Vrij, accepted in J. Colloid Interf. Sci.

[13] J. Adams, T. Baird, P.S. Braterman, J.A. Cairns and D.L. Segal, Mater. Res. Soc. 121 (1988) 361.

[14] J.K. Bailey and M.L. Mecartney, Colloids Surf. 63 (1992) 151.

[15] R.D. Badley, W.T. Ford, F.J. McEnroe and R.A. Assink, Langmuir 6 (1990) 792.

[16] G.E. Maciel and D.W. Sindorf, J. Am. Chem. Soc. 102 (1980) 7606.

[17] D.W. Sindorf and G.E. Maciel, J. Am. Chem. Soc. 105 (1983) 1487.

[18] D.W. Sindorf and G.E. Maciel, J. Am. Chem. Soc. 105 (1983) 3767.

[19] C.A. Fyfe, G.C. Gobbi and G.J. Kennedy, J. Phys. Chem. 89 (1985) 277.

[20] R.H. Glaser, G.L. Wilkes and E. Bronnimann, J. Non-Cryst. Solids 113 (1989) 73.

[21] A.J. Vega and G.W. Scherer, J. Non-Cryst. Solids 111 (1989) 153.

[22] B. Pfleiderer, K. Albert, E. Bayer, L. van de Ven, J. de Haan and C. Cramers, J. Phys. Chem. 94 (1990) 4189.

[23] R.K. Iler, The Chemistry of Silica (Wiley, New York, 1979).

[24] K. Osseo-Asare and F.J. Arriagada, Colloids Surf. 50 (1990) 321.

[25] F.J. Arriagada and K. Osseo-Asare, 'Nanosize silica via controlled hydrolysis in reverse micellar systems', paper presented at R.K. Iler Memorial Symposium, Washington, Aug. 1990, Colloids Surf., in press.

[26] W. Noll, Chemie und Technologie der Silicone, 2nd Ed. (Verlag Chemie, Weinheim, 1968) pp. 168–210, 246–287.

[27] L.H. Sommer, Stereochemistry, Mechanism and Silicon (McGraw-Hill, New York, 1965) p. 130–150.

[28] T.W. Zerda and G. Hoang, J. Non-Cryst. Solids 109 (1989) 9.

[29] T.W. Zerda and G. Hoang, Chem. Mater. 2 (1990) 372.

[30] J.L. Lippert, S.B. Melpolder and L.M. Kelts, J. Non-Cryst. Solids 104 (1988) 139.

[31] C. Fyfe, Solid State NMR for Chemists (CFC, ON, 1983).

[32] C.P. Slichter, Principles of Magnetic Resonance, 3rd Ed., updated (Springer, Berlin, 1990).

[33] W. Noll, Chemie und Technologie der Silicone, 2nd Ed. (Verlag Chemie, Weinheim, 1968) pp. 1–15.

[34] J.W. Jansen, C.G. de Kruif and A. Vrij, J. Colloid Interf. Sci. 114 (1989) 481.

[35] J.W. Jansen, thesis Rijksuniversiteit Utrecht (1986).

[36] H.G.M. Penders and A. Vrij, Colloid Polym. Sci. 268 (1990) 823.

[37] R.C. Weast, ed., Handbook of Chemistry and Physics, 56th Ed. (Chemical Rubber Co., Cleveland, OH, 1976).

[38] A.P. Philipse, C. Smits and A. Vrij, J. Colloid Interf. Sci. 129 (1989) 335.

[39] C.F. Bohren and D.R. Huffman, Absorption and Scattering of Light by Small Particles (Wiley, New York, 1983).

[40] A. van Veluwen, H.N.W. Lekkerkerker, C.G. de Kruif and A. Vrij, J. Chem. Phys. 89 (1988) 2810.

[41] R. Pecora, ed., Dynamic Light Scattering: Applications of Photon Correlation Spectroscopy (Plenum, New York, 1985).

[42] D.A. Torchia, J. Magn. Reson. 30 (1978) 613.

[43] A.P. Philipse and A. Vrij, J. Chem. Phys. 87 (1987) 5634.